Desalination and Water Treatment
www.deswater.com

doi: 10.5004/dwt.2022.28246

250 (2022) 240–251
February

Linear and nonlinear modeling of kinetics and isotherms characterizing adsorptive removal of 4-nitrophenol by biochar BC-PFP$_{773}$

Shamroza Mubarik*, Samreen Ehsan, Marryam Imran, Farzana Hanif

Department of Chemistry, Govt. Sadiq College Women University Bahawalpur 63100, Pakistan, Tel. +92 3227666144; email: shamroza.mubarik@gscwu.edu.pk (S. Mubarik), Tel. +92 3128355447; email: samreenehsan567@gmail.com (S. Ehsan), Tel. +92 3097961181; email: maryam.imranbwp@gmail.com (M. Imran), Tel. +92 3017745540; email: farzanawajid67@gmail.com (F. Hanif)

Received 24 July 2021; Accepted 22 January 2022

ABSTRACT

In this research article the batch adsorption of 4-nitrophenol on chemically treated biomaterial BC-PFP$_{773}$ was studied at three different temperatures (10°C, 20°C, 45°C). The consequences of various operating factors including biosorbent dosage, contact time and pH on the percentage removal of 4-nitrophenol was detected. The perceived optimum contact time for the adsorption of 4-nitrophenol was 60 min. The optimum biomass dosage (BC-PFP$_{773}$) was 2.5 g/L for the adsorption of 4-nitrophenol. The value of regression coefficient R^2 for first order and second-order are 0.95 and 0.99, respectively which shows that second-order is most appropriate model for determination of kinetics. Experimental results were verified by applying different linear and nonlinear isotherm models such as Langmuir, Freundlich, Temkin, Dubinin–Radushkevich, Hill, Sips, Toth, Fritz-Schlunder (4 parameters) and Fritz-Schlunder (5 parameter). The value of thermodynamic parameters, that is, $\Delta H°$ is –3.74 kJ/mol and $\Delta S°$ is 44.31 J/mol/K respectively. The thermodynamic parameters revealed the thermodynamic feasibility of the adsorption process. The negative value of $\Delta G°$ indicates the spontaneous process and the negative value of $\Delta H°$ illustrates that the process is exothermic.

Keywords: Adsorption; Pseudo-second-order; Nonlinear isotherms; Linear isotherms; 4-Nitrophenol; Thermodynamics; BC-PFP$_{773}$

1. Introduction

Swiftly increasing industrialization, unplanned urbanization and agricultural activities are mediated to be the major cause of water pollution. Numerous industrial operations engross surplus volumes of water. A few of them, peculiarly textiles, paper, pharmaceuticals and petro-chemicals re-emit effluents consisting of variability of chemicals which are lethal to humans and environment. Phenol and its derivatives encompass a class of priority pollutants as they are carcinogenic and mutagenic even at very low concentrations [1–4]. 4-nitrophenol is one of the significant intermediate used in organic synthesis. Extensive use of 4-nitrophenol is in the synthesis of two pesticides, ethyl and methyl parathion. As a fungicide for leather, in dyes, pigment production and also in specialty products for military applications. Nitro-phenols are listed as toxic pollutants by United States environmental protection agency [5,6]. Short-term exposure to the 4-nitrophenol can cause eye irritation, nausea, drowsiness and headaches. It can be absorbed by human body and convert hemoglobin to methemoglobin thereby decreasing the oxygen uptake of body [7]. The harmful effects of 4-nitrophenol on humans are due to its carcinogenic and mutagenic nature including skin diseases. 4-nitrophenol is extremely toxic and can cause impairment of liver, kidney, and nervous system. 4-nitrophenol can alternate the normal monocyte count. Several conventional technologies have been used for the phenol contaminated water

* Corresponding author.

with their related merits and demerits. Adsorption technology is now accepted as entrenched and effective to treat wastewater and activated carbons being the most adequate adsorbents because of their chemical appearance and porous structure [8,9]. Extensive reports are available on the use of agricultural wastes and by-products to prepare activated carbons through different procedures. For example; coir pith, palm stones, peanut shells, cork and coffee endocarp [10–13]. In present study petiolar felt-sheath of palm (PFP), produced as a raw material from palm trees was checked for its capability to remove 4-nitrophenol from single system.

2. Experimental set-up

2.1. Adsorbate

The commercially available well-known 4-nitrophenol (MF: $C_6H_5NO_3$) was obtained from Sigma-Aldrich and used as adsorbate. The stock solution was prepared by taking 1.0 g of 4-nitrophenol in 1,000 mL measuring flask. Dissolving and making the volume up to the mark with double distilled water. Desired concentrations were freshly prepared whenever needed.

2.2. Adsorbent

Raw material used in the current study was collected from the local market. The biomaterial investigated for adsorption studies include *Livistona chinensis*, (common name petiolar felt-sheath of palm, PFP). The given raw material was thoroughly washed under tap water to remove dust. Afterwards washed with double distilled water until the removal of coloration. Oven dried at 80°C ± 2°C for 24 h. Ground and stored in desiccators or air tight bags. For chemical pretreatment, a known amount of biomass was impregnated with HCl (1 M), HNO_3 (1 M), and H_2SO_4 (1 M) in 1:5 ratio in 500 mL Erlenmeyer flasks and shaken at a speed of 150 rpm for 24 h at room temperature. Treated biomaterials were then filtered and washed with double distilled water till the filtrate was free of acid. The pretreated biomaterial was oven dried at 80°C ± 2°C for 24 h and stored in desiccators for use in further experiments. Raw and pretreated biomaterial (1 M HCl, 1 M HNO_3 and 1 M H_2SO_4) were charred in muffle furnace (box-type resistance furnace, SX-6–12) at temperature 773 K for 30 min. The prepared biochars were investigated for their maximum adsorption aptitudes for 4-nitrophenol as target pollutant in batch and continuous flow system.

3. Results and discussion

3.1. Fourier-transform infrared spectroscopy studies

Fourier-transform infrared spectroscopy (FTIR) analysis is employed to identify the number of peaks that represent the structure of BC-PFP_{773}. Fig. 1a represents the FTIR spectra of native BC-PFP_{773}. The peaks in the range of 3,125–3,575 cm^{-1} is owing to the presence of –OH groups in the membrane. The band observed in the region of 1,725–1,750 cm^{-1} is related to C=O group (aldehydes, ketones) stretching vibrations. The band appeared in a range of 1,040–1,300 cm^{-1} is due to $–CH_3$ stretching. The band observed in the region of 1,100–1,600 cm^{-1} is related to carboxylate group.

Fig. 1b represents the FTIR spectra after adsorption of 4-nitrophenol on biomaterial BC-PFP_{773}. The peak observed at 3,347.45 cm^{-1} thus identified as O–H stretching which shifted to 3,358.02 cm^{-1} after 4-nitrophenol adsorption. The region between 1,725 and 1,750 cm^{-1} indicates the C=O stretch thus the peak appeared at 1,731.09 cm^{-1} shifted to 1,738.45 cm^{-1} indicating the change in bond energies after 4-nitrophenol adsorption. The $–CH_3$ band shifted from 1,221.17 to 1,224.3 cm^{-1}. The band observed in carboxylate region shifted from 1,601.89 to 1,603.01 cm^{-1}.

3.2. Scanning electron microscopy studies

The scanning electron microscopy images for the morphological features and surface characteristics of raw, PFP and biochars BC-PFP_{773} are presented in Figs. 2a and b. While raw PFP have rough and irregular spaces with depressions on the surface which were converted to smooth, long, deep well shaped micro tubes when charred at different temperatures. Thus conversion of rough surface of native biomaterials to highly porous structures facilitate the adsorption of 4-nitrophenol by increasing the surface area of the BC-PFP_{773}.

3.3. Effect of operating factors

3.3.1. Effect of contact time

The contact time is a key parameter which greatly influences the rate of adsorption. The adsorption rate of 4-nitrophenol was considered over a time intervals of 5–180 min by keeping adsorbent dosage 2.5 g/L with 10 mg/L 4-nitrophenol solution. It was observed from Fig. 3a that within the first 5 min 83% of 4-nitrophenol was adsorbed. However, increase in adsorption was observed up to 60 min and equilibrium condition was achieved after 60 min. The maximum percentage removal (98%) of 4-nitrophenol was observed in 1 h from the contaminated solution. The rapid uptake within the first 5 min is due to the excessive and available vacant adsorption sites on the surface of BC-PFP_{773} which became depleted as the contact time was elevated and achieved equilibrium. Where the rate of adsorption becomes equal to the rate of desorption.

3.3.2. Effect of adsorbent dosage

The influence of biochar dosage on the adsorption of 4-nitrophenol is shown in Fig. 3b. When 100 mL of 25 mg/L solution of 4-nitrophenol was agitated with various quantities of BC-PFP_{773}. The adsorption capacity of BC-PFP_{773} was increased from 48% to 100% with the rise in the dosage of BC-PFP_{773} from 0.1 g/L to 2.5 g/L. This is due to the availability of additional adsorption sites at higher biochar quantity. Further increase in biochar dosage up to 10 g/L produced negligible change in the values of percentage removal of 4-nitrophenol. This is because of the saturation of adsorbent sites as a result of decreasing mass of biochar for a fixed volume and concentration of adsorbate.

3.3.3. Effect of pH

The effect of solution pH on the removal of 4-nitrophenol was observed by varying the initial pH between the

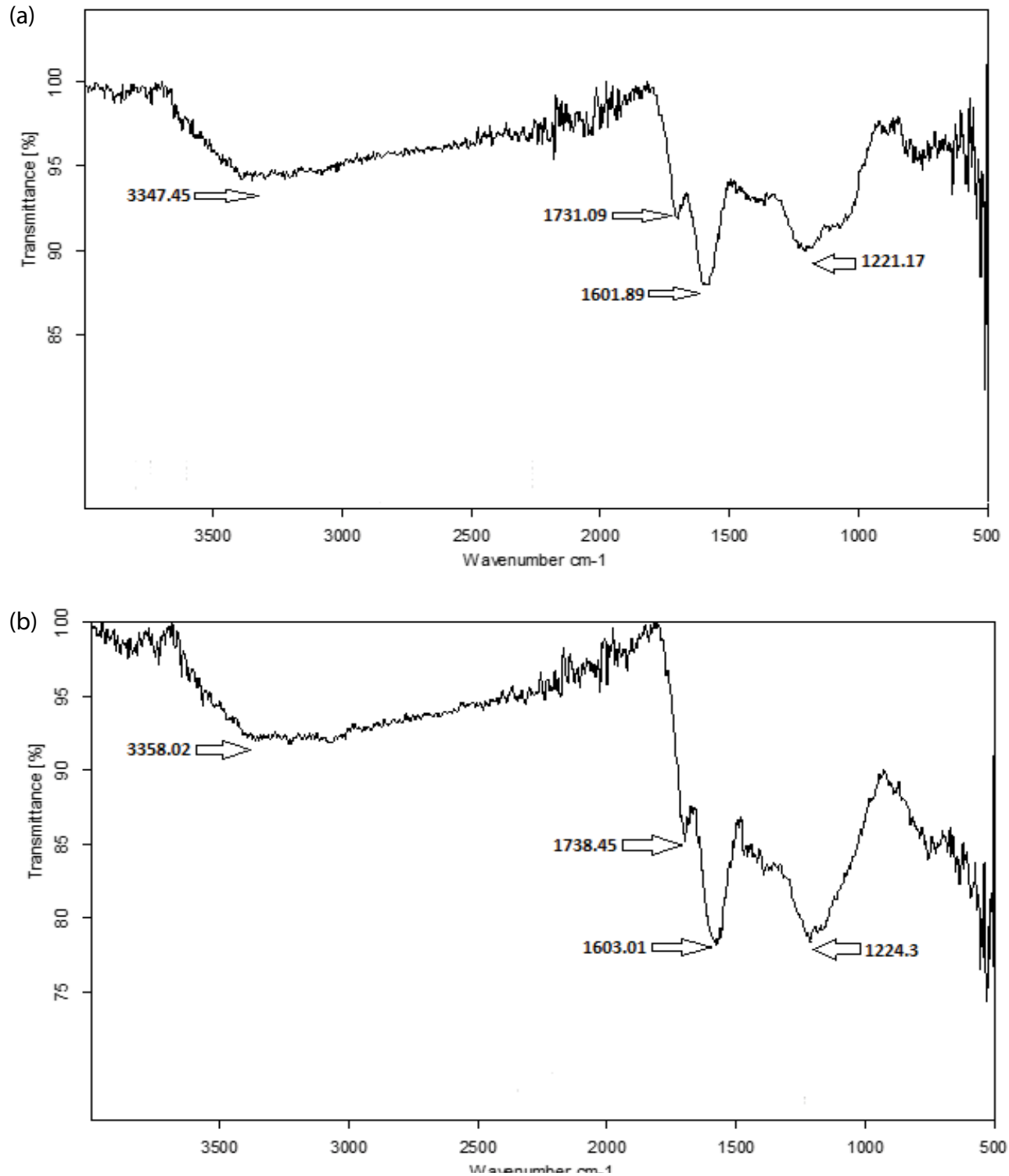

Fig. 1. FTIR spectra of (a) naked petiolar felt-sheath of palm charred at 773 K (BC-PFP$_{773}$) and (b) 4-nitrophenol loaded BC-PFP$_{773}$.

range of 2–10 (Fig. 3c). Maximum elimination of 4-nitrophenol was observed at acidic pH and remains constant upto pH 6. As pH of the solution was enhanced above 8, adsorption of 4-nitrophenol was reduced. 4-nitrophenol is soluble in water with a pK$_a$ value of 7.15. It was observed that at pH 2, 4-nitrophenol was in molecular form and there was no electrostatic repulsion between 4-nitrophenol and the surface of BC-PFP$_{773}$. The point of zero charge (pH$_{pzc}$) of BC-PFP$_{773}$ is 4.0, at a solution pH lower than pH$_{pzc}$. The total external charge on the surface of biochar will be positive while at a pH higher than pH$_{pzc}$ it is negative. At lower pH values maximum adsorption is attributed to the

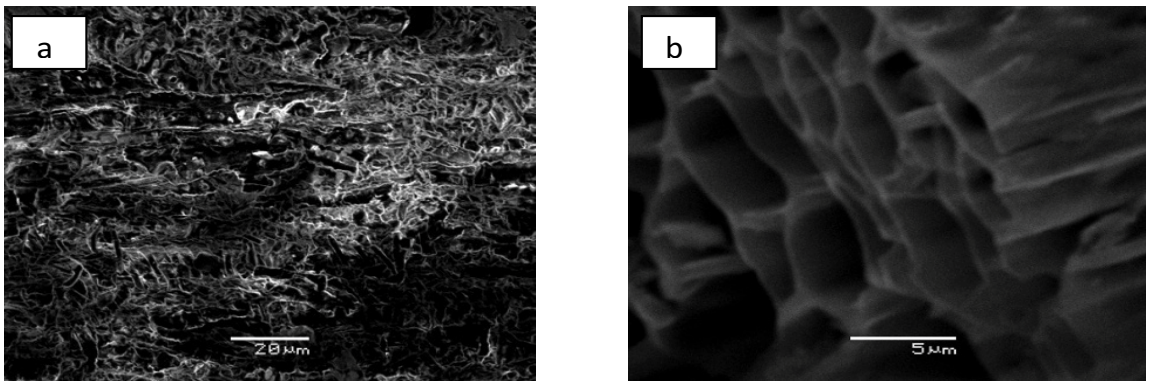

Fig. 2. Scanning electron monograph of (a) raw petiolar felt-sheath of palm (PFP) and (b) biochar produced at 773 K (BC-PFP$_{773}$).

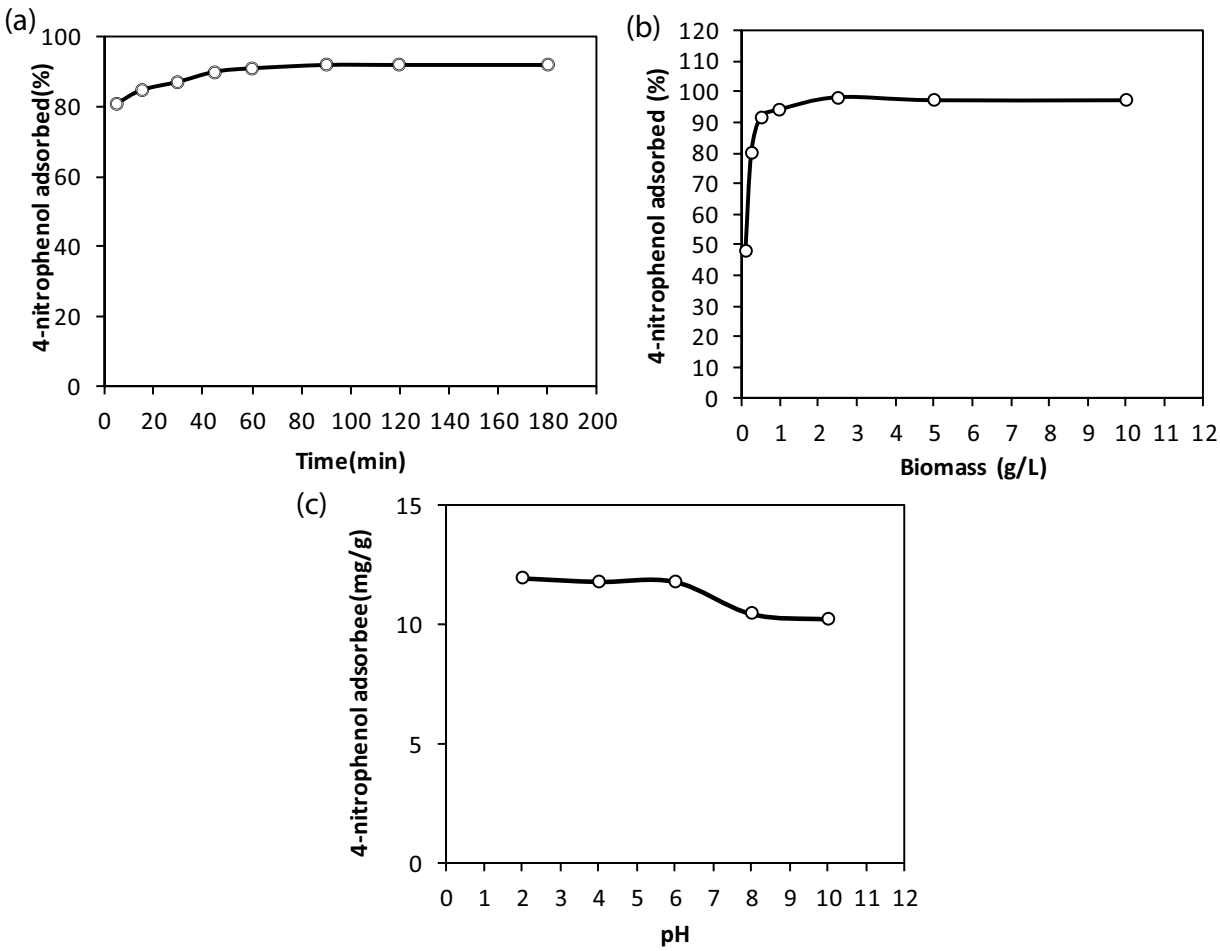

Fig. 3. (a) Effect of contact time on the removal of 4-nitrophenol by BC-PFP$_{773}$, (b) effect of biosorbent BC-PFP$_{773}$ on the removal of 4-nitrophenol, and (c) effect of pH on the removal of 4-nitrophenol.

electron donor-acceptor mechanism between lone pair of electrons on O–H group of 4-nitrophenol and the surface of biochar. At alkaline pH values (above 7) 4-nitrophenol is dissociated into its ionic form 4-nitrophenolate anion and the number of anionic sites also increased. Thus repulsion is created between negative 4-nitrophenolate anions and the negatively charged biochar surface which becomes negative at pH higher than point of zero charge. Thus a sharp decrease in the adsorption capacity of BC-PFP$_{773}$ was observed at higher pH values. Another factor contributing for decreased adsorption of 4-nitrophenol at high pH values is the presence of OH^- ions competing with 4-nitrophenolate anions for the remaining positively charged surface sites.

3.4. Adsorption kinetics

The kinetic study yields central information about the rate of uptake of adsorbate by the adsorbent.

3.4.1. Pseudo-first-order model

The expression for linearized pseudo-first-order kinetic model can be expressed as [14]:

$$\log\left(q_e - q_t\right) = \log q_e - k_1 T \tag{1}$$

The expression for non-linearization pseudo-first-order can be expressed as:

$$q_t = q_e\left(1 - e^{-k_1 T}\right) \tag{2}$$

As q_t and q_e describes the amount of adsorbed adsorbate at time t and at equilibrium respectively and k_1 is the rate constant associated with first-order kinetic model.

The expression for linearized form of pseudo-second-order kinetic model can be given as:

$$\frac{t}{q_t} = \frac{1}{k_2 q_e^2} + \frac{t}{q_e} \tag{3}$$

The non-linearized expression for pseudo-second-order can be given as:

$$q_t = \frac{K_2 q_e^2 t}{1 + K_2 q_e t} \tag{4}$$

As q_e is the amount of adsorbed adsorbate at equilibrium, q_t is the amount of the adsorbed adsorbate at equilibrium and k_2 is the rate constant associated with pseudo-second-order kinetic model [15,16].

3.4.2. Intraparticle diffusion model

The equation of intraparticle diffusion model can be expressed as:

$$q_t = K_{\text{diff}} t^{1/2} + C \tag{5}$$

where k_i is intraparticle diffusion rate constant (g/mg min) and the intercept of the plot, c stands for the boundary layer effect or surface adsorption. It was observed that the contribution of surface adsorption in rate determining step is increased as the value of intercept becomes larger. When the kinetic data was analyzed using the intraparticle diffusion model, it was observed that the plot did not pass through the origin indicating that intraparticle diffusion was not the only rate-limiting step.

K_{diff}	c	R^2
is 0.103	4.019	0.95

It was also observed that the values of intraparticle diffusion rates were lower for 4-nitrophenol than values for surface adsorption (intercept, c). The trend in these results would indicate that a higher amount of surface adsorption occurred leading to a reduction in the rate of diffusion of 4-nitrophenol from the adsorbent external surface to the internal surface

3.5. Adsorption isotherms

3.5.1. Linear isotherms

The Langmuir isotherm is usually applied to study the monolayer adsorption by homogeneous surfaces.

According to this model adsorption occur on definite number of sites which are indistinguishable but comparable. All sites are equally susceptible for the adsorbate. The expression for linear form can be given as:

$$\frac{1}{q_e} = \frac{1}{q_m} + \frac{1}{K_L q_m C_e} \tag{6}$$

$$R_L = \frac{1}{\left(1 + bC_e\right)} \tag{7}$$

where C_e is the concentration of adsorbate in solution at equilibrium, q_e refers to adsorbed adsorbate at equilibrium. A solution (mg/L) and b stands for Langmuir isotherm constant. A plot of C_e against C_e/q_e is shown in Fig. 4a and values of the parameters K_L and q_m is listed in Table 1. R_L is a dimensionless separation factor and can be given as [17].

$$R_L = \frac{1}{\left(1 + K_L C_o\right)} \tag{8}$$

where C_o = maximum initial concentration of the adsorbate (mg/L).

If $R_L > 1$ adsorption is unfavorable, If $R_L = 1$, $R_L = 0$, $0 < R_L > 1$ then adsorption is linear, irreversible and favorable respectively. The value of R_L 4-nitrophenol are 0.74, 0.632 and 0.55 for adsorption of 4-nitrophenol at temperature 10°C, 20°C and 45°C, respectively. Which reveals that adsorption is favorable? The R^2 value are 0.97, 0.99 and 0.99 for the 4-nitrophenol adsorption by BC-PFP$_{773}$ at temperature 25°C, 35°C and 45°C respectively. The R^2 value confirmed the applicability of Langmuir isotherm for these temperatures.

According to Freundlich isotherm the adsorption occurs in multilayer way. The linearized expression for Freundlich isotherm can be given as [18]:

$$\ln q_e = \ln K_f + \frac{1}{n} \ln C_c \tag{9}$$

where K_f and n are Freundlich constant, the value of n provides information about heterogeneity.

The adsorbent surface. If the value of n is 2–10 then it reveals the decent adsorption power of the adsorbent. If it is 1–2 then it shows moderate adsorption and less than one signifies reduced adsorption capability. The R^2 value for the Freundlich isotherm are 0.99, 0.98, and 0.92 for

temperature 10°C, 20°C and 45°C, respectively. The values of n are 1.59, 1.84 and 2.5 at temperature 10°C, 20°C and 45°C, respectively which shows that adsorption is more advantageous at 45°C.

The linear expression for Temkin isotherm can be given as [19]:

$$Q_e = \frac{RT}{b_t}\ln A_t + \frac{RT}{b_t}\ln C_e \tag{10}$$

3.5.2. Nonlinear isotherms

The nonlinear form of Langmuir isotherm can be expressed as:

$$q_e = \frac{q_m K_L C_e}{1 + K_L C_e} \tag{11}$$

where K_L is Langmuir constant, q_m is the adsorption capacity. The nonlinear model of Langmuir isotherm is given in Fig. 5 and values of q_m and K_L are calculated in Table 2. The value of chi-square for adsorption of nitrophenol are 10°C, 35°C, and 45°C respectively. The nonlinear form of Freundlich can be represented as $q_e = K_f C1/n$.

$$Q_e = K_F C_e^{1/n} \tag{12}$$

Table 1
Comparison of various adsorbents for adsorption of 4-nitrophenol

Adsorbent	Capacity	Reference
Petiolar felt-sheath of palm (PFP)	18	Present study
Loofah fibers	265.4	[21]
Carrot dross	125	[22]
Activated jute stick char	39.38	[23]
Empty fruit bunches (EFB)	7.54	[24]
Mesocarp fibers (MF)	9.61	[24]
Corn husk	11.668	[25]

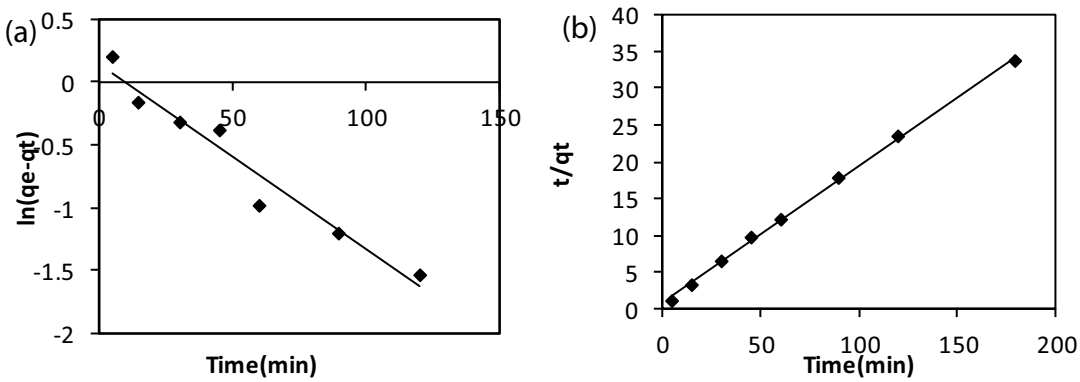

Fig. 4. Linear form of (a) pseudo-first-order kinetic model and (b) pseudo-second-order kinetic model for the adsorption of 4-nitrophenol by PFP_{773}.

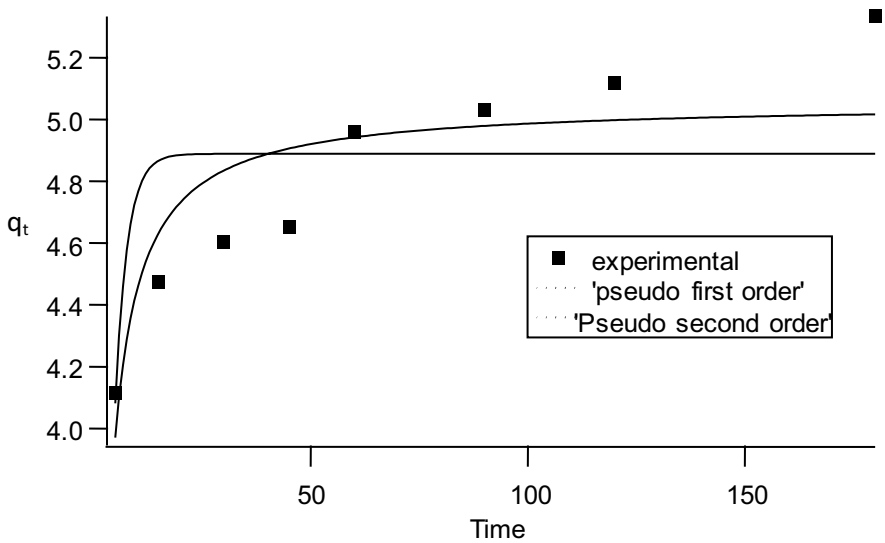

Fig. 5. Nonlinear form of pseudo-first-order and pseudo-second-order kinetic model for the adsorption of 4-nitrophenol by BC-PFP_{773}.

Table 2
Parameters of pseudo-first-order and pseudo-second-order kinetic models for adsorption of 4-nitrophenol by BC-PFP$_{773}$

Pseudo-first-order kinetic model (linear kinetic model)		Pseudo-first-order kinetic model (nonlinear kinetic model)
k_1	–0.032	0.360 ± 0.805
q_e	1.153	4.88 ± 0.17
R^2	0.95	–
χ^2	–	0.567
Pseudo-second-order kinetic model (linear kinetic model)		**Pseudo-second-order kinetic model (nonlinear model)**
k_2	0.040	0.14 ± 0.042
q_e	5.40	5.05 ± 0.103
R^2	0.99	–
χ^2	–	0.28

Table 3
Parameters of the linear forms of Langmuir, Freundlich and Temkin isotherm for the adsorption of 4-nitrophenol by BC-PFP$_{773}$

System 4-nitrophenol	10°C	20°C	45°C
Langmuir			
q_{max} (mg/g)	18	12.9	18
R_L	0.74	0.632	0.55
R^2	0.97	0.99	0.99
Freundlich			
K_f	7	0.98	2.8
n	1.59	1.84	2.5
R^2	0.99	0.98	0.92
Temkin			
b	0.98	0.61	0.8
A	0.98	0.37	0.7
R^2	0.98	0.96	0.96

where C_e is superflutant concentration at equilibrium stage, q_e is the amount of dye adsorbed at equilibrium, n and K_f are Freundlich factors and their values are given in Table 3. The value of chi-square for the adsorption of nitro phenol by BC-PFP$_{773}$ are 1.975 × 10^{-008}, 6.64 × 10^{-009} and 4.11 × 10^{-008} at 25°C, 35°C, and 45°C respectively.

The nonlinear form of Temkin isotherm can be expressed as:

$$q_e = \frac{RT}{b_t} \ln a_t C_e \tag{13}$$

where R, T, b_t and a_t represent general gas constant, absolute temperature, heat of adsorption and equilibrium binding constant correspond to maximum binding energy respectively. The nonlinear form of Temkin isotherm is expressed in Fig. 6. The value of R, T, b_t and a_t constants are calculated and given in Table 4. The value of chi-square for adsorption of nitrophenol by BC-PFP$_{773}$ are 8.7 × 10^{-009}, 2.07 × 10^{-008} and 9.48 × 10^{-009} at 10°C, 20°C and 45°C.

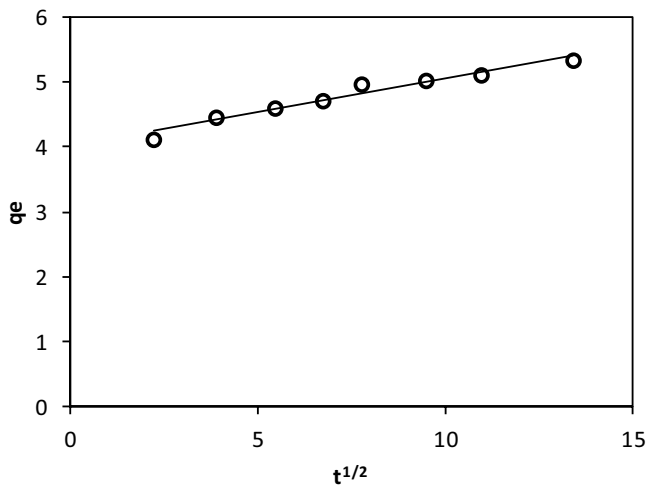

Fig. 6. Intraparticle diffusion model for the adsorption of 4-nitrophenol by BC-PFP$_{773}$.

The nonlinear form of Dubinin–Radushkevich can be represented as:

$$q_e = C_m \exp\left(-\beta\varepsilon^2\right) \tag{14}$$

The nonlinear plot of DRK is given in Fig. 7. The value of chi-square for the adsorption of nitrophenol by BC-PFP$_{773}$ are 1.33 × 10^{-008}, 9.035 ± 10^{-009} and 2.45 × 10^{-008} at 10°C, 20°C, and 45°C, respectively.

The nonlinear form of Redlich–Peterson can be represented as:

$$q_e = \frac{K_{R-P} C_e}{1 + a_{R-P} C_e^g} \tag{15}$$

The Redlich–Peterson chi-square value for the adsorption of 4-nitrophenol by BC-PFP$_{773}$ are 6.654 × 10^{-009}, 1.6 × 10^{-008} and 54.635 at 10°C, 20°C, and 45°C, respectively. The parameters for Redlich–Peterson are given in Table 4 and a nonlinear plot for this graph is represented in Fig. 8.

Table 4
Nonlinear isotherms parameters for adsorption of 4-nitrophenol by BC-PFP$_{773}$

System 4-nitrophenol	10°C	20°C	45°C
Langmuir isotherm			
K_L	701.42 ± 172	0.0011 ± 5.09 × 10^{-005}	1,349.1 ± 141
q_m	0.00961 ± 0.000	206 ± 1.56 × 10^{-010}	0.0009 ± 2.9 × 10^{-005}
χ^2	5.07 × 10^{-009}	1.26 × 10^{-008}	2.34 × 10^{-009}
Freundlich isotherm			
K_f	0.01 ± 0.006	0.011 ± 0.0065	0.006 ± 0.0026
n	2.043 ± 0.417	11.75 ± 0.306	2.73 ± 0.546
χ^2	1.975 × 10^{-008}	6.64 × 10^{-009}	4.11 × 10^{-008}
Temkin isotherm			
b	11,958 ± 1.32 × 10^{003}	1,648.4 ± 4.07 × 10^{003}	12,415 ± 773
a	7,574 ± 1.85 × 10^{003}	6,518.1 ± 4.27 × 10^{003}	15,292 ± 2.91 × 10^{003}
χ^2	8.7 × 10^{-009}	2.07 × 10^{-008}	9.48 × 10^{-009}
Dubinin–Radushkevich			
q_m	0.0022 ± 0.0005	0.002 ± 0.0006	0.0019 ± 0.000323
b	0.006 ± 0.001	0.007 ± 0.0016	0.004 ± 0.0007
χ^2	1.33 × 10^{-008}	9.035 ± 10^{-009}	2.45 × 10^{-008}
Redlich–Peterson			
K	0.95 ± 2.7 × 10^{-007}	0.329 ± 5.31 × 10^{-007}	0.473 ± 2 × 10^{-007}
a	0.55 ± 5.41 × 10^{007}	–1.064 ± 3.69 × 10^{-007}	0.14 ± 8.07 × 10^{-007}
g	0.872 ± 1.99 × 1.99 × 10^{-006}	1.299 ± 9.64 × 10^{-007}	0.721 ± 7.8 × 10^{-007}
χ^2	6.654 × 10^{-009}	1.16 × 10^{-008}	2.37 × 10^{-009}
Hill			
q_H	0.003 ± 2.56x10^{-005}	5.33 ± 157	0.003 ± 4.96x10^{-005}
n_H	0.55 ± 4.87x10^{-007}	0.568 ± 0.14	0.45 ± 7.07x10^{-007}
k_d	0.18 ± 4.27 × 10^{-007}	463 ± 1.34 × 10^{004}	0.22 ± 5.06 × 10^{-007}
χ^2	1.67 × 10^{-008}	6.64 × 10^{-009}	3.18 × 10^{-008}
Sips			
k_s	0.013 ± 6.9 × 10^{-006}	0.00066 ± 0.0028	4.303 ± 3.34
a_s	2.44 ± 4.2 × 10^{-009}	–2.4644 ± 3.17	4,661 ± 3.73 × 10^{003}
β	0.51 ± 5.37 × 10^{-007}	0.242 ± 0.42	1.14 ± 0.095
χ^2	1.82 × 10^{-008}	5.03 ± 10^{-009}	1.38 × 10^{-009}
Toth			
k_T	0.001 ± 10^{-006}	2,008 ± 7.82 × 10^{-12}	52 ± 2.84 × 10^{-009}
a_t	0.0029 ± 1.01 × 10^{-006}	1.17 ± 2.58 × 10^{-006}	1.018 ± 3.5 × 10^{-005}
t	0.6948 ± 5.25 × 10^{-008}	0.017 ± 3.36 × 10^{-005}	0.004 ± 0.00019
χ^2	3.005 × 10^{-009}	2.05 × 10^{-008}	3.12 × 10^{-008}
Fritz-Schlunder (4 parameter)			
A	0.090 ± 8.82 × 10^{-007}	0.012 ± 6.33	0.005 ± 3.87 × 10^{-005}
α	0.762 ± 4.88 × 10^{-007}	0.557 ± 15.3	0.13 ± 1.16 × 10^{-006}
B	465 ± 64 × 10^{-011}	0.11 ± 563	0.32 ± 404 × 10^{-007}
β	1.140 ± 1.67 × 10^{-007}	0.05 ± 98.11	0.32 ± 8.14 × 10^{-007}
χ^2	5.93 × 10^{-009}	6.65 × 10^{-009}	3.47 × 10^{-008}
Fritz-Schlunder (5 parameter)			
q	0.13 ± 1	0.24 ± –1	0.005 ± 4.36 × 10^{-006}
k_1	0.815 ± 1	0.19 ± –1	0.043 ± 5.62 × 10^{-006}
k_2	1,918.6 ± 1	4.23 ± 1	0.057 ± 2.14 × 10^{-006}
m_1	0.798 ± 1	–0.31 ± 1	0.081 × 1.44 × 10^{-006}
m_2	1.385 ± 1	–0.88 ± 1	0.48 ± 7.84 × 10^{-009}
χ^2	0.13 ± 1	6.65 × 10^{-009}	2.59 × 10^{-008}

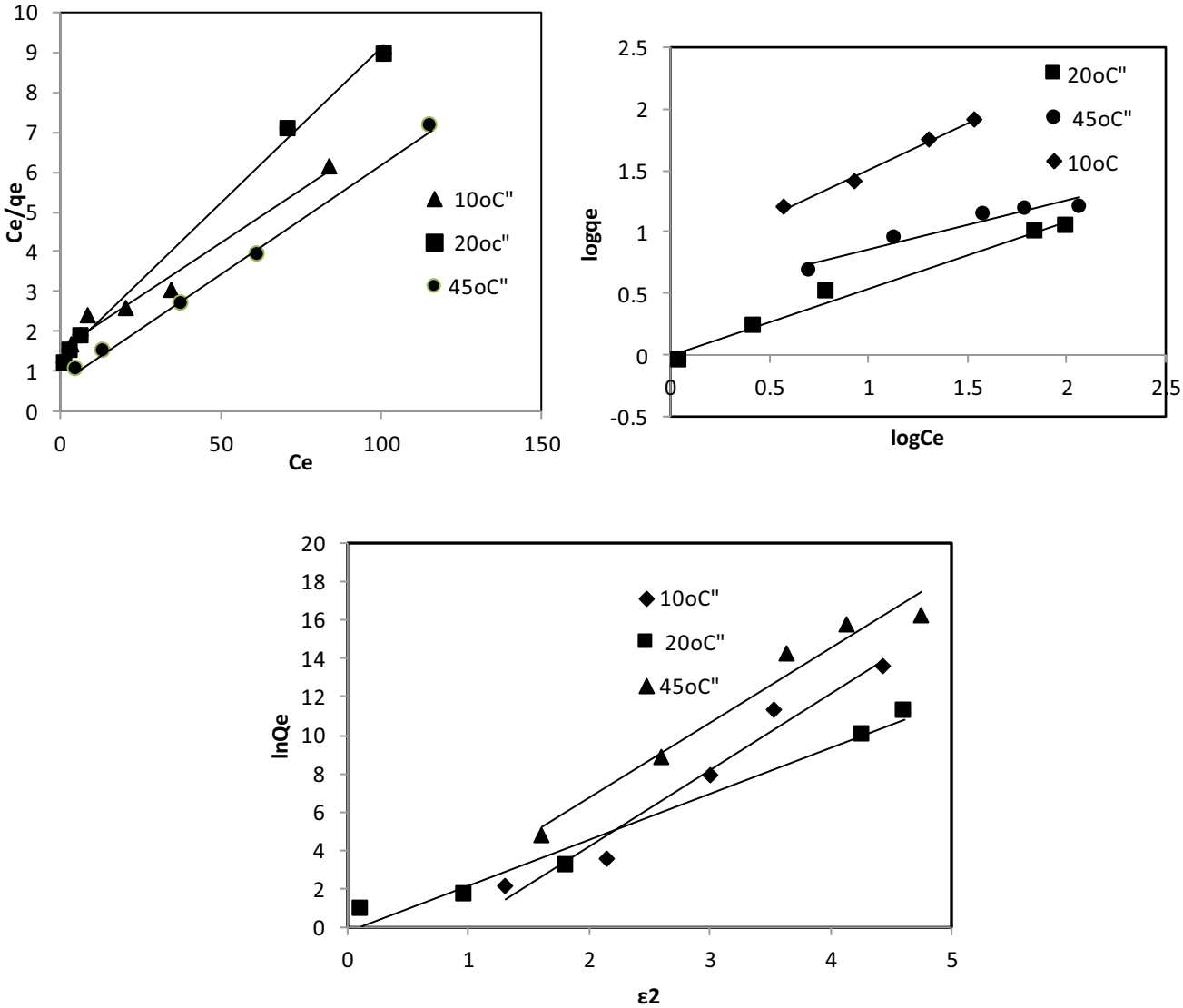

Fig. 7. Linear form of Langmuir, Freundlich and Temkin isotherm for adsorption of 4-nitrophenol by BC-PFP$_{773}$.

Sips isotherm is a combined form of both Freundlich and Langmuir isotherm. This isotherm is beneficial in case of heterogeneous surfaces. The expression of a nonlinear form of Sips isotherm is given as $q_e = k_s C_e^{\beta s}/1 + a_s C_e^{\beta s}$. At low concentration, Sips isotherm approaches to Freundlich isotherm and at high concentration, it follows Langmuir isotherm. The details of Sips parameters are given in Table 4.

The manifestation for nonlinear form of Hill can be given as [20]:

$$Q_e = \frac{q_H C_e^{n_H}}{k_H + C_e^{n_H}} \tag{16}$$

The plot for the Hill model is given in Fig. 9 and calculated constants are shown in Table 4.

The Toth isotherm is another revised from of Langmuir isotherm which is useful for the analysis of heterogeneous surfaces including both low and high boundary of adsorbate concentration. The expression for nonlinear form of Toth isotherm can be stated as:

$$q_e = \frac{k_T C_e}{\left(a_t + C_e\right)^{1/2}} \tag{17}$$

The description of Toth parameters is provided in Table 4.

3.6. Adsorption thermodynamics

The numerical values of thermodynamic parameters, that is, Gibbs free energy ($\Delta G°$), entropy ($\Delta S°$) and enthalpy ($\Delta H°$) for the adsorption of 4-nitrophenol were obtained with the help of van't Hoff equation and the related results are provided in Table 5. The graphical explanation for $\ln K_c$ vs. $1/T$ for 4-nitrophenol is given in Fig. 10. The value of Gibbs free energy is negative for the adsorption of 4-nitrophenol by BC-PFP$_{773}$ which characterizes the rise in Gibbs

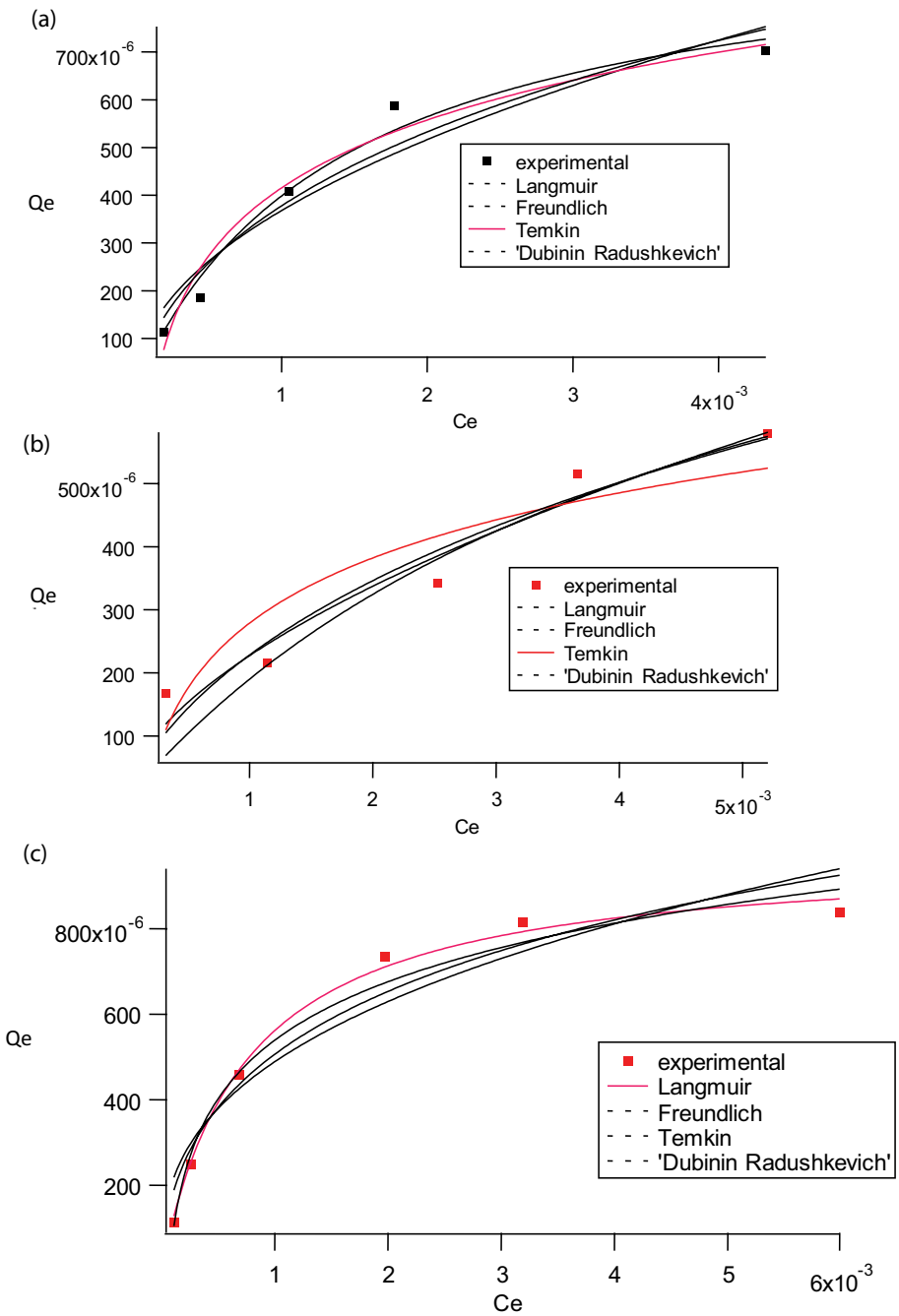

Fig. 8. Nonlinear plots of Langmuir, Freundlich, Temkin, and Dubinin–Radushkevich isotherms for the adsorption of nitrophenol by BC-PFP$_{773}$ at 10°C (a), 20°C (b), and 45°C (c).

free energy with increase in temperature. The value of $\Delta H°$ is negative which represents the adsorption of 4-nitrophenol on BC-PFP$_{773}$ is an exothermic process. The value of $\Delta S°$ is positive which proposes escalation in randomness at the interface during adsorption process.

4. Conclusion

This article explores the worth of the biochar (BC-PFP$_{773}$) for the adsorptive removal of 4-nitrophenol. The kinetic studies revealed that the value of R^2 for second-order kinetic is greater than pseudo-first-order kinetic models. The percentage removal of 4-nitrophenol was amplified with intensification in contact time and maximum adsorption attained in 1 h. The optimal biosorbent dosage for the removal of 4-nitrophenol was 2.5 g/L. Thermodynamic parameters showed that adsorption of 4-nitrophenol by BC-PFP$_{773}$ was exothermic and spontaneous process. The present research is highly efficient for the practicable synthesis of cost-effective, porous carbon based materials for the

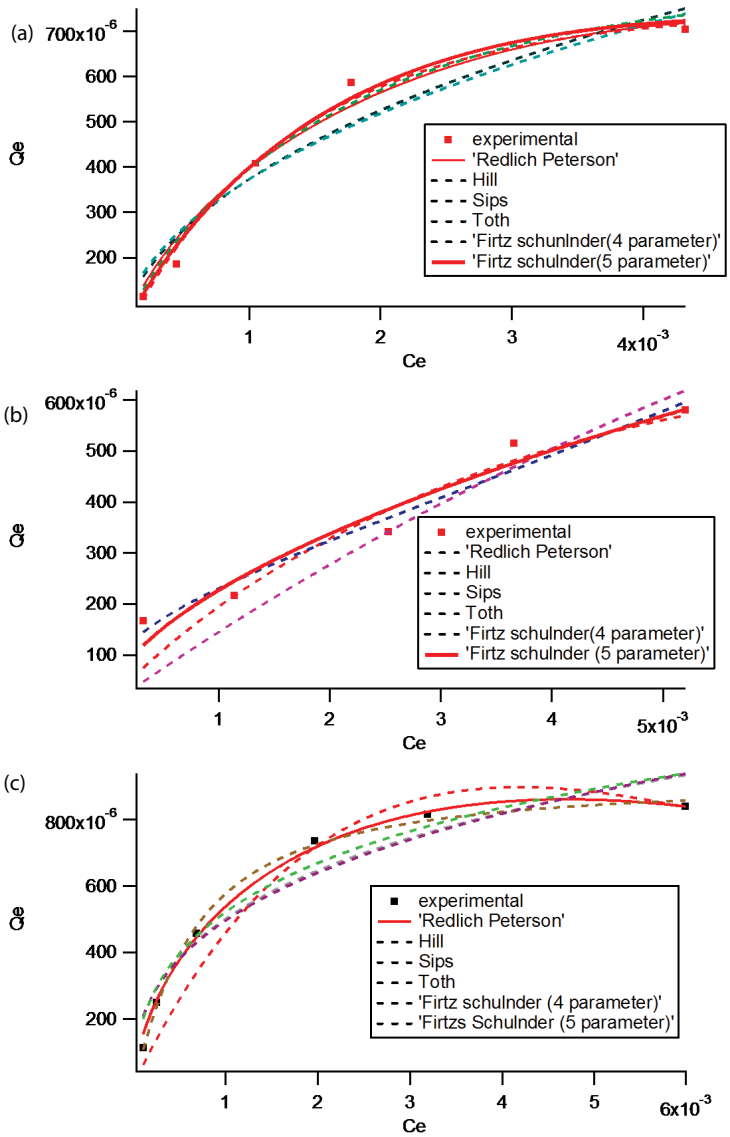

Fig. 9. Nonlinear plots of Langmuir, Freundlich, Temkin, and Dubinin–Radushkevich isotherms for the adsorption of 4-nitrophenol by BC-PFP$_{773}$ at 10°C (a), 20°C (b), and 45°C (c).

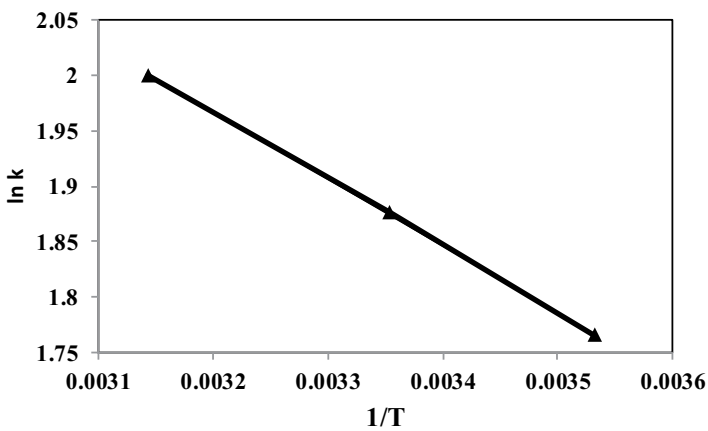

Fig. 10. The plot of 1/T vs. ln$K$ for the adsorption of 4-nitrophenol by BC-PFP$_{773}$.

Table 5
Thermodynamic parameters for adsorption of 4-nitrophenol by $BC\text{-}PFP_{773}$

$\Delta H°$ (kJ/mol)	$\Delta S°$ (J/mol/K)	$-\Delta G°$ (kJ/mol)		
		298	308	318
–3.74	44.31	16.91	17.35	17.79

elimination of organic pollutants from industrial/domestic effluents, which is crucial from environmental viewpoint. From this study it was concluded that the $BC\text{-}PFP_{773}$ can be effectively used for the treatment of waste water.

References

[1] P. Bhatia, M. Nath, Green synthesis of p-NiO/n-ZnO nanocomposites: excellent adsorbent for removal of Congo red and efficient catalyst for reduction of 4-nitrophenol present in wastewater, J. Water Process Eng., 33 (2020) 101017, doi: 10.1016/j.jwpe.2019.101017.

[2] S.R. Manippady, A. Singh, B.M. Basavaraja, A.K. Samal, S. Srivastava, M. Saxena, Iron–carbon hybrid magnetic nanosheets for adsorption-removal of organic dyes and 4-nitrophenol from aqueous solution, ACS Appl. Nano Mater., 3 (2020) 1571–1582.

[3] N. Alhokbany, T. Ahama, Ruksana, Mu. Naushad, S.M. Alshehri, AgNPs embedded N-doped highly porous carbon derived from chitosan based hydrogel as catalysts for the reduction of 4-nitrophenol, Compos. Part B, 173 (2019) 106950, doi: 10.1016/j.compositesb.2019.106950.

[4] M. Guzmán, M. Estrada, S. Miridonov, A. Simakov, Synthesis of cerium oxide (IV) hollow nanospheres with tunable structure and their performance in the 4-nitrophenol adsorption, Microporous Mesoporous Mater., 278 (2019) 241–250.

[5] J. Luo, Y. Gao, K. Tan, W. Wei, X. Liu, Preparation of a magnetic molecularly imprinted graphene composite highly adsorbent for 4-nitrophenol in aqueous medium, ACS Sustainable Chem. Eng.,4 (2016) 3316–3326.

[6] P. Cyganowski, D. Jermakowicz-Bartkowiak, A. Lesniewicz, P. Pohl, A. Dzimitrowicz, Highly efficient and convenient nanocomposite catalysts produced using *in-situ* approach for decomposition of 4-nitrophenol, Colloids Surf., A, 590 (2020) 124452, doi: 10.1016/j.colsurfa.2020.124452.

[7] H.N. Abdelhamid, High performance and ultrafast reduction of 4-nitrophenol using metal-organic frameworks, J. Environ. Chem. Eng., 9 (2020) 104404, doi: 10.1016/j.jece.2020.104404.

[8] P.T. Dhorabe, D.H. Lataye, R.S. Ingole, Removal of 4-nitrophenol from aqueous solution by adsorption onto activated carbon prepared from *Acacia glauca* sawdust, Water Sci. Technol., 73 (2016) 955–966.

[9] A. Kumar, S. Kumar, S. Kumar, D.V. Gupta, Adsorption of phenol and 4-nitrophenol on granular activated carbon in basal salt medium: equilibrium and kinetics, J. Hazard. Mater., 147 (2007) 155–166.

[10] L.C.A. Oliveira, E. Pereira, I.R. Guimaraes, A. Vallone, M. Pereira, J.P. Mesquita, K. Sapag, Preparation of activated carbons from coffee husks utilizing $FeCl_3$ and $ZnCl_2$ as activating agents, J. Hazard. Mater., 165 (2009) 87–94.

[11] J. Georgin, G.L. Dotto, M.A. Mazutti, E.L. Foletto, Preparation of activated carbon from peanut shell by conventional pyrolysis and microwave irradiation-pyrolysis to remove organic dyes from aqueous solutions, J. Environ. Chem. Eng., 4 (2016) 266–275.

[12] B. Cardoso, A.S. Mestre, A.P. Carvalho, J. Pires, Activated carbon derived from cork powder waste by KOH activation: preparation, characterization, and VOCs adsorption, Ind. Eng. Chem. Res., 47 (2008) 5841–5846.

[13] A.C. Lua, J. Guo, Preparation and characterization of activated carbons from oil-palm stones for gas-phase adsorption, Colloids Surf., A, 179 (2001) 151–162.

[14] M.M. Karthika, M. Vasuki, Adsorption of Alizarine Red-S dye from aqueous solution by cane sugar bagasse: resolution of isotherm, kinetic and thermodynamics, Int. J. Appl. Eng. Res., 13 (2018) 10260–10267.

[15] P. Ganguly, R. Sarkhel, P. Das, Synthesis of pyrolyzed biochar and its application for dye removal: batch, kinetic and isotherm with linear and non-linear mathematical analysis, Surf. Interfaces, 20 (2020) 100616, doi: 10.1016/j.surfin.2020.100616.

[16] F. Batool, J. Akbar, S. Iqbal, S. Noreen, S.N.A. Bukhari, Study of isothermal, kinetic, and thermodynamic parameters for adsorption of cadmium: an overview of linear and nonlinear approach and error analysis, Bioinorg. Chem. Appl., 2018 (2018) 3463724, doi: 10.1155/2018/3463724.

[17] S. Akazdam, M. Chafi, W. Yassine, B. Gourich, Removal of acid orange 7 dye from aqueous solution using the exchange resin amberlite FPA-98 as an efficient absorbent: kinetics, isotherms, and thermodynamics study, J. Mater. Environ. Sci., 8 (2017) 2993–3012.

[18] C.A. Başar, Applicability of the various adsorption models of three dyes adsorption onto activated carbon prepared waste apricot, J. Hazard. Mater., 135 (2006) 232–241.

[19] H. Masood, S. Zafar, H. ur Rehman, M.I. Khan, H.B. Ahmad, A. Naz, W. Hassan, M.H. Lashari, Adsorptive removal of anionic dyes in aqueous binary mixture by anion exchange membrane, Desal. Water Treat., 194 (2020) 248–258.

[20] A.V. Hill, The possible effects of the aggregation of the molecules of haemoglobin on its dissociation curves, J. Physiol., 40 (1910) 4–7.

[21] M. Salimi, Z. Salehi, H. Heidari, F. Vahabzadeh, Production of activated biochar from *Luffa cylindrica* and its application for adsorption of 4-nitrophenol, J. Environ. Chem. Eng., 9 (2021) 105403, doi: 10.1016/j.jece.2021.105403.

[22] T.R. Bastami, M.H. Entezari, Activated carbon from carrot dross combined with magnetite nanoparticles for the efficient removal of p-nitrophenol from aqueous solution, Chem. Eng. J., 210 (2012) 510–519.

[23] M. Ahmaruzzaman, S. Laxmi Gayatri, Batch adsorption of 4-nitrophenol by acid activated jute stick char: equilibrium, kinetic and thermodynamic studies, Chem. Eng. J., 158 (2010) 173–180.

[24] L. Baloo, M.H. Isa, N.B. Sapari, A.H. Jagaba, L.J. Wei, S. Yavari, R. Razali, R. Vasu, Adsorptive removal of methylene blue and acid orange 10 dyes from aqueous solutions using oil palm wastes-derived activated carbons, Alexandria Eng. J., 60 (2021) 5611–5629.

[25] S. Mishra, S.S. Yadav, S. Rawat, J. Singh, J.R. Koduru, Corn husk derived magnetized activated carbon for the removal of phenol and para-nitrophenol from aqueous solution: interaction mechanism, insights on adsorbent characteristics, and isothermal, kinetic and thermodynamic properties, J. Environ. Manage., 246 (2019) 362–373.